CHEMISTRY

Homoatomic cations: From $[P_5]^+$ to $[P_9]^+$

Julia Frötschel-Rittmeyer[1], Michael Holthausen[1], Christian Friedmann[2], David Röhner[2], Ingo Krossing[2]*, Jan J. Weigand[1]*

Recent synthetic approaches to a series of $[P_9]X$ salts ($X = [F\{Al(OR^F)_3\}_2]$, $[Al(OR^F)_4]$, and ($R^F = C(CF_3)_3$); Ga_2Cl_7) overcome limitations in classical synthesis methods that proved unsuitable for phosphorus cations. These salts contain the homopolyatomic cation $[P_9]^+$ via (I) oxidation of P_4 with $NO[F\{Al(OR^F)_3\}_2]$, (II) the arene-stabilized Co(I) sandwich complex $[Co(arene)_2][Al(OR^F)_4]$ [arene = *ortho*-difluorobenzene (*o*-DFB) and fluorobenzene (FB)], or (III) the reduction of $[P_5Cl_2][Ga_2Cl_7]$ with $Ga[Ga_2Cl_7]$ as Ga(I) source in the presence of P_4. Quantum chemical CCSD(T) calculations suggest that $[P_9]^+$ formation from $[Co(arene)_2]^+$ occurs via the nido-type cluster $[(o\text{-DFB})CoP_4]^+$, which resembles the isoelectronic, elusive $[P_5]^+$. Apparently, the nido-cation $[P_5]^+$ forms intermediately in all reactions, particularly during the Ga(I)-induced reduction of $[P_5Cl_2]^+$ and the subsequent pick up of P_4 to yield the final salt $[P_9][Ga_2Cl_7]$. The solid-state structure of $[P_9][Ga_2Cl_7]$ reveals the anticipated D_{2d}-symmetric Zintl-type cage for the $[P_9]^+$ cation. Our approaches show great potential to bring other $[P_n]^+$ cations from the gas to the condensed phase.

INTRODUCTION

Intensely colored oleum solutions of nonmetallic homopolyatomic cations of sulfur, selenium, and tellurium were likely the first examples for this elusive cation class and were observed as early as around 1800 (*1*). However, the first real evidence for representatives began with the synthesis and characterization of $[O_2][PtF_6]$ in 1962 (*2*, *3*), and many more examples of homoatomic cations of most nonmetallic elements have been isolated and characterized in the solid state in the past 60 years excluding examples of crystal structures of homoatomic phosphorus cations. For the latter element, experimental and theoretical work showed that it is possible to generate pure polyphosphorus cations in the gas phase (*4*). Moreover, Martin *et al.* (*5*) observed larger $[P_n]^+$ cations (n = 2 to 24) in the gas phase by mass spectrometric studies as early as 1986, with cation $[P_{91}]^+$ being the largest to date (*6*). More recent calculations suggest the smaller, odd-numbered cluster cations $[P_n]^+$ with n up to 15 to be the most approachable in the condensed phase (*7*). The first evidence for the existence of $[P_9]^+$ in the condensed phase was published only in 2012: The oxidant $[NO][Al(OR^F)_4]$ ($R^F = C(CF_3)_3$) reacts with an excess of P_4 (*8*) to the C_{2v}-symmetric $[P_4NO]^+$ cation, which acts toward P_4 as a "P^+" donor. Very likely, the elusive $[P_5]^+$ cation is formed and acts as an intermediate, which subsequently adds a second molecule P_4 to yield $[P_9]^+$ (Fig. 1, I).

RESULTS AND DISCUSSION

The aforementioned reaction has been studied in quite some detail, and despite the use of the larger and more robust weakly coordinating anion $[F\{Al(OR^F)_3\}_2]^-$ in route I (Fig. 1) (*9*), it was not possible so far to crystallize any $[P_9]^+$ cation salt $[P_9]X$ ($X = [F\{Al(OR^F)_3\}_2]$, $[Al(OR^F)_4]$; cf. table S5 and figs. S7 to S11). Nevertheless, the amorphous salt $[P_9][F\{Al(OR^F)_3\}_2]$ obtained in 1,2,3,4-tetrafluorobenzene (4FB) as reaction medium in 69% yield reversibly dissolves in this solvent and shows a superior long-time stability of over 40 days, which is fundamentally different to the corresponding $[Al(OR^F)_4]$ salt and allows stoichiometric reactions in the future.

From a retrosynthetic point of view and realizing that $[P_5]^+$ plays a pivotal role in the synthesis of $[P_9]^+$, we developed two new approaches. This includes the new reaction pathway II toward $[P_9][Al(OR^F)_4]$ via oxidation of white phosphorus with the "naked" Co(I) sandwich cations $[Co(arene)_2][Al(OR^F)_4]$ [arene = *ortho*-difluorobenzene (*o*-DFB) (*10*) and fluorobenzene (FB)], which was confirmed by nuclear magnetic resonance (NMR) spectroscopy (Fig. 1, II). Quantum chemical calculations suggest occurrence of a nido-cluster intermediate $[(o\text{-DFB})CoP_4]^+$ that resembles the isoelectronic $[P_5]^+$ (cf. figs. S36 and S37). The crude nonmagnetic black by-product was analyzed by powder diffraction [powder x-ray diffraction (pXRD)] and energy-dispersive x-ray (EDX) measurements. The analysis agrees with its tentative assignment as the well-known cobalt phosphide CoP_3 (cf. fig. S22). (*11*–*13*)

Recent years gave access to cationic polyphosphorus compounds such as $[P_5X_2]^+$ (X = Br, I) (*14*) and $[P_5R_2]^+$ (R = alkyl, aryl) (*15*–*17*). Hence, for the most successful route III, particularly cation $[P_5Cl_2]^+$ in combination with an adequate reducing agent that turned out to be the best $[P_5]^+$ synthon (Fig. 1, III). However, the synthesis of a $[Al(OR^F)_4]^-$ salt containing the cation $[P_5Cl_2]^+$ following the reported procedure for the Br and I analogs only led to mixtures. By contrast, it succeeds as the salt $[P_5Cl_2][GaCl_4]$, when P_4 is reacted in PCl_3 as the reaction medium with the required stoichiometric amount of $GaCl_3$ at room temperature. $[P_5Cl_2][GaCl_4]$ can be isolated as colorless solid in excellent yields (86%) and starts to decompose in solution (CH_2Cl_2, FB, and *o*-DFB) and in the solid state at room temperature in the course of a few hours (solution) up to a few days (solid material) to P_4, $GaCl_3$, PCl_3, and an insoluble orange solid of unknown constitution, likely Schenck-type phosphorus (*18*). However, when stored in the dark and at −30°C, the salt is stable for several weeks. The molecular structure of $[P_5Cl_2]^+$ was confirmed by single-crystal x-ray structure determination of the more stable $[P_5Cl_2][Ga_2Cl_7]$ salt (cf. table S12 and fig. S23). The optimized synthesis of $[P_9][Ga_2Cl_7]$ requires the slow treatment of $[P_5Cl_2][GaCl_4]$ with $GaCl_3$ and $Ga[Ga_2Cl_7]$ as reducing agent, in the presence of a huge excess of P_4 (10.0 equivalents), and a 5:1 solvent mixture of FB and CS_2 as reaction medium (Fig. 1, III).

[1]Faculty of Chemistry and Food Chemistry, Technische Universität Dresden, 01062 Dresden, Germany. [2]Institut für Anorganische und Analytische Chemie and Freiburg Materials Research Center FMF, Albert-Ludwigs-Universität Freiburg, Albertstrasse 21, 79104 Freiburg, Germany.
*Corresponding author. Email: jan.weigand@tu-dresden.de (J.J.W.); krossing@uni-freiburg.de (I.K.)

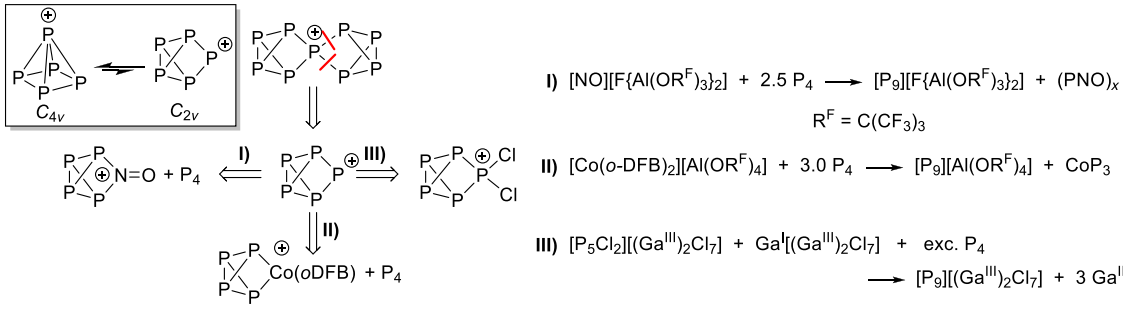

Fig. 1. Retrosynthesis concepts toward $[P_9]^+$ and preparation of salts $[P_9]X$. (**I**) $X = [F\{Al(OR^F)_3\}_2]$: P_4 (2.5 equivalents), $NO[F\{Al(OR^F)_3\}_2]$ (1.0 equivalents), RT, exclusion of light, 4FB, (68%). (**II**) $X = [Al(OR^F)_4]$: P_4 (3.0 equivalents), $[Co(o\text{-}DFB)_2][Al(OR^F)_4]$ (1.0 equivalents), RT, FB, (21%). (**III**) $X = [Ga_2Cl_7]$: P_4 (10.0 equivalents), $[P_5Cl_2][Ga_2Cl_7]$ (1.0 equivalents), $Ga[Ga_2Cl_7]$ (1.0 equivalents), RT, FB/CS_2, (77%). R^F, $C(CF_3)_3$.

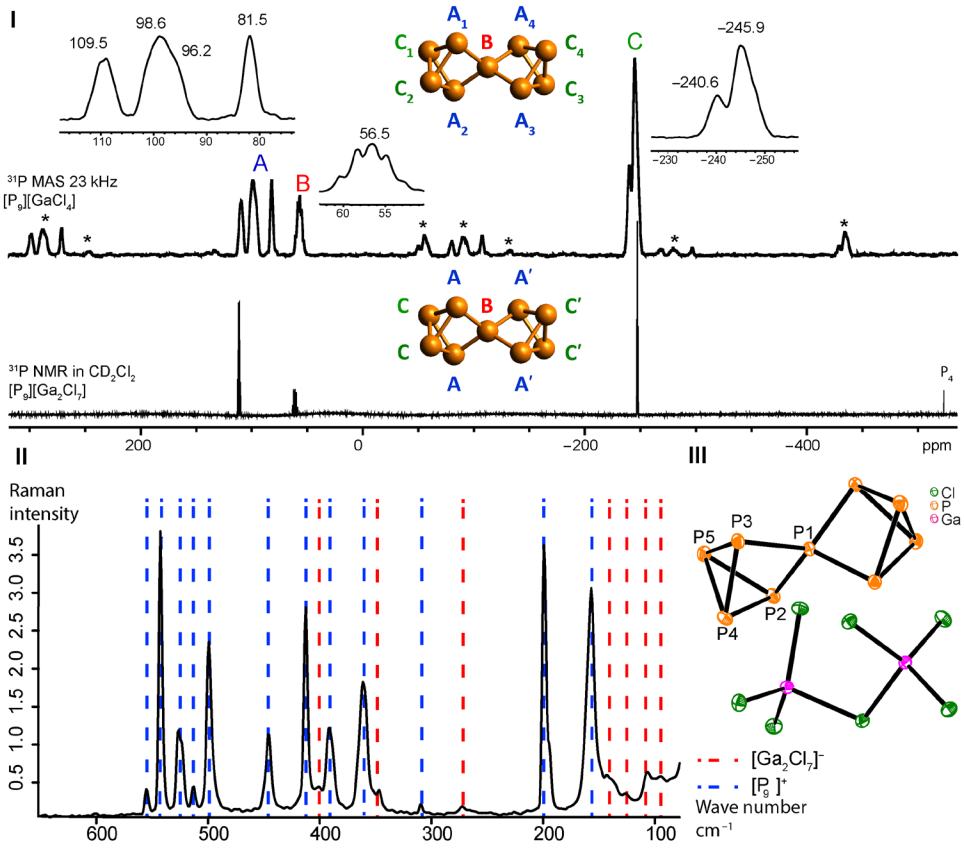

Fig. 2. Characterization of $[P_9][Ga_2Cl_7]$. (**I**) ^{31}P MAS NMR and liquid $^{31}P\{^1H\}$ NMR spectra of the separated crystals in CD_2Cl_2; asterisks (*) denote spinning sidebands in the MAS NMR. (**II**) Raman spectrum and assignment. (**III**) Molecular structure of cation $[P_9]^+$ including anion $[Ga_2Cl_7]^-$.

Typically, the dissolved Ga(I) source $Ga[Ga_2Cl_7]$ in FB is added dropwise to the FB/CS_2 solution of $[P_5Cl_2][GaCl_4]$, $GaCl_3$, and P_4 over the course of 30 min, leading to the precipitation of $[P_9][Ga_2Cl_7]$ as an orange microcrystalline material in 77% yield. Salt $[P_9][Ga_2Cl_7]$ is stable when stored at low temperature (−35°C) for a long period of time (several month) but starts to decompose when heated above 60°C readily [simultaneous thermal analyzer (STA) measurement; see fig. S6]. The excess of P_4 can be conveniently and quantitatively recovered from the reaction medium. The purity of solid $[P_9][Ga_2Cl_7]$ was confirmed by ^{31}P MAS (magic angle spinning) NMR spectroscopy and Raman spectroscopy (Fig. 2, I and II), elemental analysis [inductively coupled plasma (ICP)], and pXRD (figs. S5 and S26). The salt is poorly soluble in common solvents such as CH_2Cl_2, FB, and *o*-DFB, but sufficiently concentrated solutions for liquid NMR studies and crystal preparations can be obtained by addition of small amounts of $GaCl_3$. Note that if the reduction is performed without CS_2 and only stoichiometric amounts of P_4 are present, then the formation of a much smaller amount of $[P_9]^+$ is observed in the reaction mixture that is, however, sufficiently concentrated for NMR studies in solution. The solution of ^{31}P NMR spectrum of dissolved

crystalline $[P_9][Ga_2Cl_7]$ reveals the expected $A_2A'_2BC_2C'_2$ spin system with signals at δ_A = 111.31 parts per million (ppm), δ_B = 60.91 ppm, and δ_C = −247.49 ppm. The chemical shifts and coupling constants retrieved from the iteration of the $^{31}P\{^1H\}$ NMR spectrum compare well to all the aforementioned $[P_9^+]$ salts (Fig. 2, I; fig. S5; and tables S1 and S2).

Suitable crystals for XRD were obtained by overlaying either reaction solutions without CS_2 (polymorph 1, space group $P2_1/n$) or concentrated solutions of $[P_9][Ga_2Cl_7]$ with additional $GaCl_3$ in *o*-DFB (polymorph 2, space group $I2/a$) with *n*-pentane at −30°C (Fig. 2, III, and cf. the Supplementary Materials). The second polymorph shows half of the salt composition in the asymmetric unit, and the P—P bond lengths of $[P_9]^+$ compare well to those observed in related $[P_5X_2]^+$ (X = Br, I) (*14*) and $[P_5R_2]^+$ (R = alkyl, aryl) (*15*–*17*) cations. Similarly, the transannular P—P bond [P4–P5: 2.1871 (7) Å] is found to be the shortest, followed by the P—P bonds connected to the tetracoordinate P-unit [P1–P2: 2.1902 (6) Å and P1–P3: 2.1991 (5) Å]. The remaining P—P bonds show an average length of 2.239 Å (Fig. 2, III). The composition of the $[P_9]^+$ cation shows the anticipated approximate D_{2d}-symmetric Zintl-type cage structure with slightly divergent bond and dihedral angles very likely caused by the stronger interaction of the cation with the $[Ga_2Cl_7]^-$ anion. A Hirshfeld plot and fingerprint analysis confirm this stronger intramolecular interaction and also further explain the chemically nonequivalent phosphorus atoms in solid state and, thus, the rather complex ^{31}P MAS spectrum (Fig. 2, I; table S15; and figs. S27 to S29). The pXRD diffractogram of the microcrystalline $[P_9][Ga_2Cl_7]$ compares well with the simulated powder diffraction pattern of the second polymorph (cf. fig. S26) and indicates that the solid sample is phase pure.

To gain a deeper insight into the formation mechanism of $[P_9][Ga_2Cl_7]$, quantum chemical calculations were performed at the (RI-)B3LYP(D3BJ)/def2-TZVPP level for structure optimizations and calculation of conductor-like polarizable continuum model (CPCM)-Gibbs solvation energies in 5:1 FB:CS_2 solution. The energies of all particles were refined at the rather definitive DLPNO-CCSD(T)/QZVPP level with ORCA 5. Because ^{71}Ga-NMR spectroscopy proved the presence of $[Ga^I(FB)_2]^+$ in $Ga^I[(Ga^{III})_2Cl_7]$ solutions in FB (fig. S30) (*19*–*21*), the starting point for the formation of $[P_9]^+$ (Fig. 3) is the ion pairing reaction (Fig. 3, 1) of $[Ga^I(FB)_2]^+$ with the $[Ga^{III}Cl_4]^-$ counterion from $[P_5Cl_2][Ga^{III}Cl_4]$, the strongest Lewis base in the system, to give salt $[(FB)Ga^IGa^{III}Cl_4]$ ($\Delta_RG_{(solv)}$ = −59.4 kJ mol^{-1}) with Ga(I) and Ga(III) centers. Excess $Ga^{III}Cl_3$ leads to the formation of the observed counter anion $[(Ga^{III})_2Cl_7]^-$, which, however, is known to equilibrate readily in arene solution with $[Ga^{III}Cl_4]^-$ and $Ga^{III}Cl_3$ (*22*). The ion pair $[(FB)Ga^IGa^{III}Cl_4]$ then oxidatively adds via the Ga(I) ion into one of the two identical P—Cl bonds of $[P_5Cl_2]^+$ (Fig. 3, 2), liberates the FB molecule, and forms $[ClP_5(Ga^{III})_2Cl_5]^+$ ($\Delta_RG_{(solv)}$ = −75.0 kJ mol^{-1}). This P-coordinated P_5Cl adduct to the very strong chloride acceptor $[(Ga^{III})_2Cl_5]^+$ reacts by a rearrangement reaction (Fig. 3, 3) via intermediate Cl coordination to give $[P_5]^+$ under separation of neutral $(Ga^{III})_2Cl_6$ [$\Delta_RG_{(solv)}$ = −19.7 kJ mol^{-1}]. The $[P_5]^+$ intermediate generated picks up free P_4, which is present in a huge excess, to give the final product $[P_9]^+$ [$\Delta_RG_{(solv)}$ = −43.8 kJ mol^{-1}] in an oxidative addition (Fig. 3, 4). With excess $(Ga^{III})_2Cl_6$ in the solution, it crystallizes as salt $[P_9][(Ga^{III})_2Cl_7]$, facilitated by the rather low solubility of the formed salt. The suggested entire reaction path is highly exergonic by −197.9 kJ mol^{-1}, and although we evaluated alternative reaction paths as well, the one described here appears most likely to us (cf. the Supplementary Materials). However, all likely reaction pathways include the elusive $[P_5]^+$ as intermediate (Fig. 1, retrosynthesis).

With the crystal structure of $[P_9][Ga_2Cl_7]$, the present work provides the first structural confirmation of a homopolyatomic phosphorus cation. The successful implementation of new synthetic strategies and a detailed elucidation of the possible reaction pathways showcase the elusive $[P_5]^+$ as an intermediate, isoelectronic to the putative cyclopentadienyl cation ($C_5H_5^+$) (*23*). The transition from the planar cyclic organic cation toward the Wade'ian nido type (*24*) was calculated to occur even by the substitution of only one CH group for the entire series $[(HC)_xP_{5-x}]^+$, with x = 0 to 4 by Green and

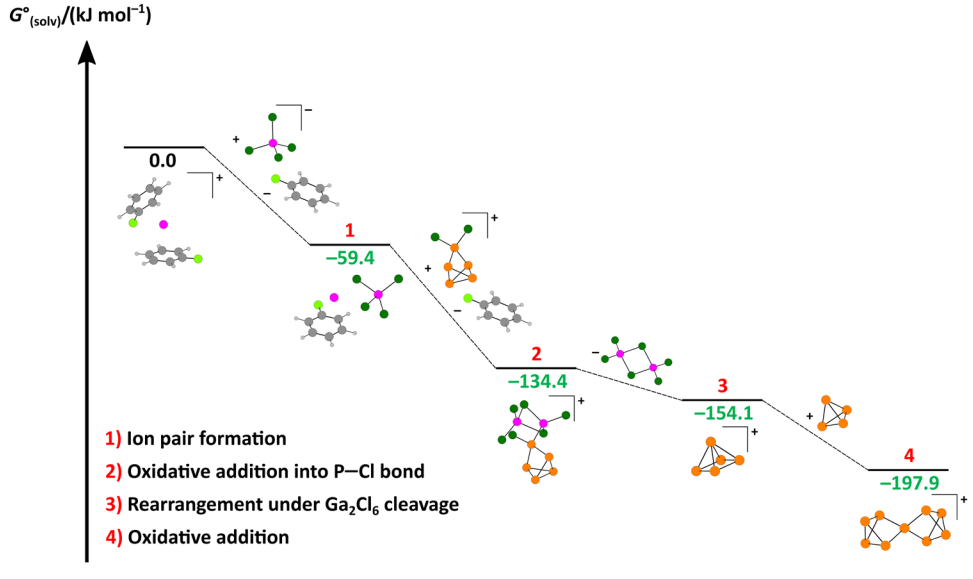

Fig. 3. Calculated mechanism toward the formation of $[P_9]^+$ starting from $[P_5Cl_2][Ga^{III}Cl_4]$, P_4, and in situ formed $[Ga^I(FB)_2][(Ga^{III})_2Cl_7]$. Geometry optimization was performed at the (RI-)B3LYP(D3BJ)/def2-TZVPP level of theory, and single-point energies were calculated at the DLPNO-CCSD(T)/QZVPP level with ORCA. Solvation corrections were calculated in FB:CS_2 (v/v, 5:1), with the CPCM model (ε_r = 5.2) at the B3LYP(D3BJ)/def2-TZVPP level of theory.

colleagues (*25*). However, only the synthesis of [3,5-tBu$_2$-1,2,4-C_2P_3][$AlCl_4$] was reported by Russell and colleagues (*26*, *27*) so far. Now, the elusive $[P_5]^+$ has also strong evidence to be present in condensed phases, and our synthetic strategies pave the way for the discovery of further novel molecules.

MATERIALS AND METHODS

General remarks for $[P_9][Ga_2Cl_7]$

Manipulations were performed in a Glovebox MB UNIlab or using Schlenk techniques under an atmosphere of purified nitrogen or argon, respectively. Dry, oxygen-free solvents (CH_2Cl_2, FB, *o*-DFB, and CS_2; distilled from CaH_2), and *n*-hexane and *n*-pentane (distilled from potassium) were used. Deuterated benzene (C_6D_6) was distilled from potassium. Deuterated dichloromethane (CD_2Cl_2) was dried over molecular sieve. All distilled and deuterated solvents were stored over molecular sieves (4 Å: CH_2Cl_2, CD_2Cl_2, FB, *o*-DFB, C_6D_6, *n*-hexane, *n*-pentane, and CS_2). All glassware were oven-dried at 160°C before use. Ga[Ga_2Cl_7] was purchased from Shanghai Richem International. All NMR measurements were performed with the Bruker AVANCE III HD Nanobay, 400-MHz UltraSield [^{1}H (400.13 MHz), ^{13}C (100.61 MHz), ^{31}P (161.98 MHz), and ^{71}Ga (122.03 MHz)] equipped with a BBFO probe or on a Bruker AVANCE III HDX, 500-MHz Ascend [^{1}H (500.13 MHz), ^{13}C (125.75 MHz), ^{31}P (202.45 MHz), and ^{71}Ga (152.52 MHz)] equipped with a BBO Prodigy CryoProbe. Chemical shifts were referenced to δ_{TMS} = 0.00 ppm (^{1}H and ^{13}C, externally) and $\delta_{H3PO4(85\%)}$ = 0.00 ppm (^{31}P, externally). Chemical shifts (δ) are reported in parts per million. Coupling constants (*J*) are reported in hertz. ^{31}P solid-state NMR spectra were recorded on a BRUKER Avance 300-MHz spectrometer using a commercial 2.5-mm MAS NMR probe and operating at a resonance frequency of 121.5 MHz. The MAS frequency was 15 and 23 kHz. $NaH_2PO_4{\cdot}H_2O$ was used as an external standard. Melting points were recorded on an electrothermal melting point apparatus (Büchi, Switzerland, Melting Point M-560) in sealed capillaries under argon atmosphere and are uncorrected. Infrared (IR) and Raman spectra were recorded at ambient temperature using a Bruker Vertex 70 instrument equipped with a RAM II module (Nd-YAG laser, 1064 nm). The Raman intensities are reported in percent relative to the most intense peak and are given in parenthesis. An attenuated total reflection (ATR) unit (diamond) was used for recording IR spectra. The intensities are reported relative to the most intense peak and are given in parenthesis using the following abbreviations: ≥0.8 = very strong (vs), ≥0.6 = strong (s), ≥0.4 = medium (m), ≥0.2 = weak (w), and ≤0.2 = very weak (vw). Elemental analysis and the Ga, P content were determined by ICP–optical emission spectrometry (OES) on an Optima 2000 DV (PerkinElmer), calibrated to two wave numbers for P (213.6 and 214.9 nm) and Ga (294.4 and 417.2 nm). Therefore, [P_9][Ga_2Cl_7] was digested in 5 ml of 100% HNO_3 with further heating at 120°C for 10 min. The STA measurement was performed on a STA 8000 (PerkinElmer) under argon atmosphere (25 ml min^{-1}) within a temperature range from 35° to 600°C (10 K min^{-1}).The ^{31}P{^{1}H} spectra of compounds [P_9][Ga_2Cl_7] were fitted using the full line shape iteration of gNMR software (*28*) to determine the ^{31}P—^{31}P coupling constants.

Synthesis of $[P_5Cl_2][GaCl_4]$

A solution of $GaCl_3$ (710 mg, 4 mmol) in PCl_3 (7 ml) was added to a suspension of P_4 (500 mg, 4 mmol) in PCl_3 (5 ml). The reaction was stirred under exclusion of light for 1 hour at ambient temperature. After the addition of *n*-hexane (20 ml), a pale yellow precipitate was formed, which was filtered, washed with *n*-hexane (5 ml), and dried in vacuo to yield $[P_5Cl_2][GaCl_4]$ as pale yellow, light sensitive, and pyrophoric solid in 86% yield (1.5 g). $[P_5Cl_2][GaCl_4]$ decomposes in solution and slowly in the solid state when stored at room temperature to P_4, $GaCl_3$, PCl_3, and an insoluble orange solid material of unknown constitution. Figure S2 shows the ^{31}P NMR spectrum of dissolved $[P_5Cl_2][GaCl_4]$ in CD_2Cl_2 after 4 hours, indicating its decomposition. When stored at −30°C under the exclusion of light, solid $[P_5Cl_2][GaCl_4]$ is stable for at least 3 months. ^{31}P NMR (202.45 MHz, CD_2Cl_2, 300 K): δ = 148.7 ppm [2P, dt, $^1J(P_BP_A)$ = −341 Hz, $^1J(P_CP_A)$ = −142 Hz, P_A, $[P_5Cl_2]^+$], 56.2 ppm [1P, tt, $^1J(P_BP_A)$ = −341 Hz, $^2J(P_CP_B)$ = 27 Hz, P_B, $[P_5Cl_2]^+$], and −269.2 ppm [2P, td, $^1J(P_CP_A)$ = −142 Hz, $^2J(P_CP_B)$ = 27 Hz, P_C, $[P_5Cl_2]^+$]. Raman (100 mW, 298 K): ν = 594 cm^{-1} (10), 562 cm^{-1} (13), 537 cm^{-1} (100), 435 cm^{-1} (33), 415 cm^{-1} (69), 392 cm^{-1} (26), 382 cm^{-1} (20), 357 cm^{-1} (38), 339 cm^{-1} (59), 262 cm^{-1} (23), 227 cm^{-1} (18), 182 cm^{-1} (51), 151 cm^{-1} (24), 132 cm^{-1} (18), and 118 cm^{-1} (14). IR (ATR, 298 K): ν = 1212 cm^{-1} (w), 630 cm^{-1} (w), 585 cm^{-1} (vs), 564 cm^{-1} (s), 552 cm^{-1} (vs), 536 cm^{-1} (vs), and 412 cm^{-1} (vs). Elemental analysis (solvent free): GaP_5Cl_6 calculated: N: 0.00, C: 0.00, H: 0.00; found: N: 0.03, C: 0.32; H: 0.01. Melting point: 62–64°C (decomposition).

Synthesis of $[P_5Cl_2][Ga_2Cl_7]$

$GaCl_3$ (528 mg, 3.0 mmol) in PCl_3 (3 ml) was added to P_4 (124 mg, 1.0 mmol). The mixture was stirred for 1 hour at ambient temperature under the exclusion of light. A colorless precipitate formed within 5 min. Converted to a colorless oil. The supernatant was decanted from the oil and washed with *n*-hexane (3 × 5 ml), and all volatiles were removed in vacuo leaving pure $[P_5Cl_2][Ga_2Cl_7]$ as colorless microcrystaline material in 92% yield (599 mg). Dissolved and solid $[P_5Cl_2][Ga_2Cl_7]$ also decomposes to P_4, $GaCl_3$, PCl_3 and an insoluble orange solid. It is also much longer stable in the dark at −30°C at least for several month. Crystals suitable for x-ray analysis can be grown from concentrated CH_2Cl_2 solution layered with *n*-pentane at −30°C. ^{31}P NMR (202.45 MHz, CD_2Cl_2, 300 K): δ = 149.1 ppm [2P, dt, $^1J(P_BP_A)$ = −340 Hz, $^1J(P_CP_A)$ = −143 Hz, P_A, and $[P_5Cl_2]^+$], 56.2 ppm [1P, tt, $^1J(P_BP_A)$ = −340 Hz, $^2J(P_CP_B)$ = 27 Hz P_B, $[P_5Cl_2]^+$], and −269.3 ppm [2P, td, $^1J(P_CP_A)$ = −143 Hz, $^2J(P_CP_B)$ = 27 Hz, P_C, and $[P_5Cl_2]^+$]. Raman (100 mW, 298 K): ν = 595 cm^{-1} (15), 564 cm^{-1} (14), 540 cm^{-1} (100), 437 cm^{-1} (37), 420 cm^{-1} (59), 393 cm^{-1} (42), 363 cm^{-1} (80), 339 cm^{-1} (30), 276 cm^{-1} (12), 264 cm^{-1} (29), 227 cm^{-1} (22), 181 cm^{-1} (54), 152 cm^{-1} (20), 135 cm^{-1} (43), and 102 cm^{-1} (31). IR (ATR, 298 K): ν = 1189 cm^{-1} (m), 637 cm^{-1} (w), 590 cm^{-1} (vs), 562 cm^{-1} (vs), and 539 cm^{-1} (vs). Elemental analysis (solvent free): $Ga_2P_5Cl_9$ calculated: N: 0.00, C: 0.00, and H: 0.00; found: N: 0.03, C: 0.40, and H: 0.144. Melting point: 52° to 55°C (decomposition).

Synthesis of $[P_9][Ga_2Cl_7]$

P_4 (140 mg, 1.2 mmol, 10 equivalents) dissolved in 1 ml of CS_2 was added to a solution of $[P_5Cl_2][GaCl_4]$ (50 mg, 0.12 mmol, 1 equivalents) and $GaCl_3$ (21 mg, 0.12 mmol, 1 equivalents) in 2 ml of FB. Ga[Ga_2Cl_7] (54 mg, 0.12 mmol, 1 equivalents) dissolved in 1.5 ml of FB was added dropwise over a period of 30 min accompanied with the formation of a pale orange powder. The suspension was filtered, and the precipitate washed with 1 ml of CS_2 and 2 ml of *n*-pentane. After drying in vacuo, [P_9][Ga_2Cl_7] was obtained as orange microcrystalline powder in 77% yield (61 mg), which was characterized by ^{31}P MAS spectroscopy, pXRD, IR, Raman, and ICP (vide infra). Note

that, from the filtrate, the excess of P_4 can be quantitatively recovered by sublimation. The filtrate contains $[P_9][Ga_2Cl_7]$, P_4, and $Cl_3POGaCl_3$ (fig. S3), of which the latter was identified by single-crystal x-ray analysis. We believe that the formation of $Cl_3POGaCl_3$ is a result of the presence of either very low amounts of moisture or the reaction of PCl_3 with the glass surface of the reaction vessels in the presence of the strong Lewis acid $GaCl_3$. This was independently confirmed by the diffusion of *n*-pentane in a solution of $GaCl_3$ in PCl_3 at −30°C, which leads to the deposition of colorless crystalline $Cl_3POGaCl_3$. The ^{31}P NMR spectrum of the $GaCl_3/PCl_3$ solution is depicted in fig. S4 and the molecular structure is depicted in fig. S19. Note that $[P_9][Ga_2Cl_7]$ is also obtained without additional $GaCl_3$, however, with a slightly decreased yield of 70%. $^{31}P\{^1H\}$ NMR (202.45 MHz, CD_2Cl_2 + $GaCl_3$, 300 K): δ = 111.5 ppm (4P, m, P_A, $[P_9]^+$), 61.0 ppm (1P, m, P_B, $[P_9]^+$), and −247.4 ppm (4P, m, P_C, $[P_9]^+$). IR (ATR, 298 K): ν = 554 cm^{-1} (m), 523 cm^{-1} (vs), and 501 cm^{-1} (s). Raman (100 mW, 298 K): ν = 555 cm^{-1} (11), 542 cm^{-1} (100), 525 cm^{-1} (32), 513 cm^{-1} (12), 498 cm^{-1} (62), 446 cm^{-1} (30), 429 cm^{-1} (5), 412 cm^{-1} (74), 401 cm^{-1} (12), 391 cm^{-1} (32), 361 cm^{-1} (48), 347 cm^{-1} (10), 309 cm^{-1} (6), 272 cm^{-1} (5), 198 cm^{-1} (96), 157 cm^{-1} (80), 143 cm^{-1} (16), 126 cm^{-1} (9), 106 cm^{-1} (17), and 95 cm^{-1} (15) (assignment; see table S3). Melting point: Compound starts to decompose at temperature above 60°C. Elemental analysis with ICP-OES: calculated: P: 41.83 and Ga: 20.93; found: P: 41.92 and Ga: 20.41.

General remarks for $[P_9][F\{Al(OR^F)_3\}_2]$ and $[P_9][Al(OR^F)_4]$ ($R^F = C(CF_3)_3$)

All reactions were performed with standard Schlenk technique in special double Schlenk flasks with G4 frit and polytetrafluoroethylene valves (fig. S1) under argon atmosphere or in gloveboxes filled with argon (O_2 and H_2O < 1 ppm) or nitrogen (O_2 and H_2O < 0.1 ppm). *o*-DFB, 1,3-difluorobenzene (*m*-DFB), 4FB, FB, and CD_2Cl_2 were dried with CaH_2, distilled, and degassed. *N*-pentane and CH_2Cl_2 were dried using a conventional MBraun Grubbs apparatus. $Co_2(CO)_8$ (1 to 10% in hexane) was used as received. $[Co(FB)_2][Al(OR^F)_4]$, $[Co(o\text{-}DFB)_2][Al(OR^F)_4]$, $[Ag][Al(OR^F)_4]$, and $[NO][F\{Al(OR^F)_3\}_2]$ were synthesized according to literature (*9*, *10*, *29*). All NMR measurements were performed with a Bruker Avance II Widebore 400-MHz, a Bruker Avance III HD 300-MHz, or a Bruker Avance 200-MHz NMR spectrometer. All NMR samples were prepared using Schlenk technique or a glovebox. All spectra were processed with the software package TopSpin 3.6.2. ^1H NMR spectra were calibrated using solvent signals versus tetramethylsilane (TMS) [*o*-DFB = 6.965 ppm, *m*-DFB = 7.082 ppm, 4FB = 6.974 ppm, and CH_2Cl_2 (relative to CD_2Cl_2) = 5.33] (*30*). The NMR spectra of other nuclei (^{19}F, ^{27}Al, and ^{31}P) were calibrated with respect to TMS using the Ξ tables from IUPAC (*31*). Simulated NMR spectra were processed using the corresponding experimental chemical shifts and iterated literature known coupling constants (*8*). CV measurements were performed with a BioLogic Science Instruments potentiostat, and the data were processed with EC-Lab software V11.21 and OriginPro 2020. Element composition was determined using a Hitachi FEGHRSEM SU8220 with a Bruker XFlash FlatQUAD detector. The measurements were performed with an acceleration voltage of 15 kV and a working distance of 17 mm.

Experimental details for $[P_9][F\{Al(OR^F)_3\}_2]$

The following synthesis in 4FB typify for all other used solvents (CH_2Cl_2, *o*-DFB, and *m*-DFB). Inside, a glovebox P_4 (81 mg, 0.7 mmol, 2.5 equivalents) and $[NO][F\{Al(OR^F)_3\}_2]$ (399 mg, 0.26 mmol, 1.0 eq.) were weighed in one side of a double Schlenk tube. Under reverse flow of argon, 4FB (4 ml) was added to the solids. Immediately, a dark red color of the solution was observed. The solution itself was stirred for at least 3 days in the dark. During this period, the color of the solution changed to yellow or orange, depending on the amount of solvent used for the reaction. The solution was filtered through the frit to the other side of the double Schlenk tube, and the solvent was slowly removed under reduced pressure. The desired product (320 mg, 0.18 mmol, 69%) was obtained as a yellowish powder and was characterized solely by NMR, because $[P_9]^+$ and $[F\{Al(OR^F)_3\}_2]^-$ are already known from literature (*8*, *9*). ^1H NMR (400.17 MHz, 4FB, 298 K): only solvent signal at 6.97 ppm. ^{19}F NMR (376.54 MHz, 4FB, 298 K): δ = −76.1 ppm (s, 54F, $[F\{Al(OC(CF_3)_3)_3\}_2]^-$) and −184.8 ppm (br. s, 1F, $[F\{Al(OC(CF_3)_3)_3\}_2]^-$). ^{27}Al NMR (104.27 MHz, 4FB, 298 K): δ = ~32 ppm (br. s, 1Al, $[F\{Al(OC(CF_3)_3)_3\}_2]^-$). ^{31}P NMR (161.99 MHz, 4FB, 298 K): δ = 123.2 ppm (m, 4P, P_A, $[P_9]^+$), 69.2 ppm (m, 1P, P_B, $[P_9]^+$), and −263.2 ppm (m, 4P, P_C, $[P_9]^+$). Note the small impurities of unknown compounds at 50.5 and −236.2.

Experimental details for $[P_9][Al(OR^F)_4]$ via $[Co(arene)_2][Al(OR^F)_4]$

The synthesis is equally feasible with arene = *o*-DFB or FB and is therefore only described for FB: In a special double Schlenk flask with G4 frit, P_4 (31 mg, 0.25 mmol, 3.0 equivalents) and $[Co(FB)_2][Al(OR^F)_4]$ (102.0 mg, 0.0837 mmol) were dissolved in FB (2 ml) and stirred for 1 hour. The solution immediately turned into a black suspension with a black precipitate. This precipitate was further analyzed by EDX and pXRD (vide supra). After filtration, the solvent was removed, and the residue was extracted with *n*-pentane (3 × 5 ml). A brownish powder (42 mg, 0.034 mmol, 21%) was obtained and analyzed by NMR spectroscopy (fig. S12 to S15). ^1H NMR (300.18 MHz, *o*-DFB, 298 K): only solvent signal at 6.97 ppm (m, *o*-DFB). ^{19}F NMR (282.45 MHz, *o*-DFB, 298 K): δ = −75.1 ppm (s, 36 F, $[Al(OC(CF_3)_3)_4]^-$), −76.1 ppm (s, $(F_3C)_3COH$), and −139.4 ppm (m, *o*-DFB). ^{27}Al NMR (78.22 MHz, *o*-DFB, 298 K): δ = 35.1 ppm (s, 1 Al, $[Al(OC(CF_3)_3)_4]^-$). ^{31}P NMR (121.51 MHz, *o*-DFB, 298 K): δ = 116.8 ppm (m, 4 P, P_A, $[P_9]^+$), 63.7 ppm (m, 1 P, P_B, $[P_9]^+$), and −261.2 ppm (m, 4 P, P_C, $[P_9]^+$).

SUPPLEMENTARY MATERIALS

Supplementary material for this article is available at https://science.org/doi/10.1126/sciadv.abq8613

REFERENCES AND NOTES

1. R. J. Gillespie, J. Passmore, Polycations of group VI. *Acc. Chem. Res.* **4**, 413–419 (1971).
2. N. Bartlett, D. H. Lohmann, Fluorides of the noble metals. Part II. Dioxygenyl hexafluoroplatinate(V), $O_2^+[PtF_6]^-$. *J. Chem. Soc.* **1962**, 5253–5261 (1962).
3. N. Bartlett, D. H. Lohmann, Dioxygenyl hexafluoroplatinate(V) $O_2^+[PtF_6]^-$. *Proc. Chem. Soc.*, 115–116 (1962).
4. P. Ballone, R. O. Jones, Density functional study of phosphorus and arsenic clusters using local and nonlocal energy functionals. *J. Chem. Phys.* **100**, 4941–4946 (1994).
5. T. P. Martin, Compound clusters. *Z. Phys. D.* **3**, 211–217 (1986).
6. A. V. Bulgakov, O. F. Bobrenok, V. I. Kosyakov, Laser ablation synthesis of phosphorus clusters. *Chem. Phys. Lett.* **320**, 19–25 (2000).
7. T. Xue, J. Luo, S. Shen, F. Li, J. Zhao, Lowest-energy structures of cationic P_{2m+1}^+ (m=1–12) clusters from first-principles simulated annealing. *Chem. Phys. Lett.* **485**, 26–30 (2010).
8. T. Köchner, T. A. Engesser, H. Scherer, D. A. Plattner, A. Steffani, I. Krossing, $[P_9]^+[Al(OR^F)_4]^-$, the salt of a homopolyatomic phosphorus cation. *Angew. Chem. Int. Ed.* **51**, 6529–6531 (2012).
9. A. Martens, P. Weis, M. C. Krummer, M. Kreuzer, A. Meierhöfer, S. C. Meier, J. Bohnenberger, H. Scherer, I. Riddlestone, I. Krossing, Facile and systematic access

to the least-coordinating WCA $[(R^FO)_3Al\text{-}F\text{-}Al(O^FR)_3]^-$ and its more Lewis-basic brother $[F\text{-}Al(OR^F)_3]^-$ ($R^F = C(CF_3)_3$). *Chem. Sci.* **9**, 7058–7068 (2018).
10. S. C. Meier, A. Holz, J. Kulenkampff, A. Schmidt, D. Kratzert, D. Himmel, D. Schmitz, E. W. Scheidt, W. Scherer, C. Bülow, M. Timm, R. Lindblad, S. T. Akin, V. Zamudio-Bayer, B. von Issendorff, M. A. Duncan, J. T. Lau, I. Krossing, Access to the bis-benzene cobalt(I) sandwich cation and its derivatives: Synthons for a "naked" cobalt(I) source? *Angew. Chem. Int. Ed.* **57**, 9310–9314 (2018).
11. J. Ackermann, A. Wold, The preparation and characterization of the cobalt skutterudites CoP_3, $CoAs_3$ and $CoSb_3$. *J. Phys. Chem. Solid* **38**, 1013–1016 (1977).
12. M. Llunell, P. Alemany, S. Alvarez, V. P. Zhukov, A. Vernes, Electronic structure and bonding in skutterudite-type phosphides. *Phys. Rev. B* **53**, 10605–10609 (1996).
13. H. D. Lutz, G. Kliche, Gitterschwingungsspektren. XXIII. IR-spektroskopische Untersuchungen an Verbindungen des Skutterudit-Typs MX_3 (M = Co, Rh, Ir; X = P, As, Sb). *Z. Anorg. Allg. Chem.* **480**, 105–116 (1981).
14. I. Krossing, I. Raabe, $P_5X_2^+$ (X=Br, I), a phosphorus-rich binary P–X cation with a C_{2v}-symmetric P_5 cage. *Angew. Chem. Int. Ed.* **40**, 4406–4409 (2001).
15. M. H. Holthausen, A. Hepp, J. J. Weigand, Synthesis of cationic $R_2P_5^+$ cages and subsequent chalcogenation reactions. *Chem.-Eur. J.* **19**, 9895–9907 (2013).
16. J. J. Weigand, M. Holthausen, R. Fröhlich, Formation of $Ph_2P_5^+$, $Ph_4P_6^{2+}$, and $Ph_6P_7^{3+}$ cationic clusters by consecutive insertions of Ph_2P^+ into P-P bonds of the P_4 tetrahedron. *Angew. Chem. Int. Ed. Engl.* **48**, 295–298 (2009).
17. M. Donath, F. Hennersdorf, J. J. Weigand, Recent highlights in mixed-coordinate oligophosphorus chemistry. *Chem. Soc. Rev.* **45**, 1145–1172 (2016).
18. R. Schenck, Über den roten Phosphor. *Z. Elektrotech. Elektrochem.* **11**, 117–118 (1905).
19. J. M. Slattery, A. Higelin, T. Bayer, I. Krossing, A simple route to univalent gallium salts of weakly coordinating anions. *Angew. Chem. Int. Ed.* **49**, 3228–3231 (2010).
20. R. J. Wehmschulte, R. Peverati, D. R. Powell, Convenient access to gallium(I) cations through hydrogen elimination from cationic gallium(III) hydrides. *Inorg. Chem.* **58**, 12441–12445 (2019).
21. M. R. Lichtenthaler, A. Higelin, A. Kraft, S. Hughes, A. Steffani, D. A. Plattner, J. M. Slattery, I. Krossing, Univalent gallium salts of weakly coordinating anions: Effective initiators/catalysts for the synthesis of highly reactive polyisobutylene. *Organometallics.* **32**, 6725–6735 (2013).
22. J. J. Weigand, N. Burford, A. Decken, The binary $Ph_2PCl/GaCl_3$ system: A room-temperature molten medium for P–P bond formation. *Eur. J. Inorg. Chem.* **2008**, 4343–4347 (2008).
23. J. B. Lambert, L. Lin, V. Rassolov, The stable pentamethylcyclopentadienyl cation. *Angew. Chem. Int. Ed.* **41**, 1429–1431 (2002).
24. K. Wade, in *Advances in Inorganic Chemistry and Radiochemistry*, H. J. Emeléus, A. G. Sharpe, Eds. (Academic Press, 1976), vol. 18, pp. 1–66.
25. D. A. Pantazis, J. E. McGrady, J. M. Lynam, C. A. Russell, M. Green, Structure and bonding in the isoelectronic series $C_nH_nP_{5-n}^+$: Is phosphorus a carbon copy? *Dalton Trans.* **2004**, 2080–2086 (2004).
26. C. Fish, M. Green, J. C. Jeffery, R. J. Kilby, J. M. Lynam, J. E. McGrady, D. A. Pantazis, C. A. Russell, C. E. Willans, Cationic phosphorus-carbon-pnictogen cages isolobal to $C_5R_5^+$. *Chem. Commun.*, 1375–1377 (2006).
27. J. M. Lynam, M. C. Copsey, M. Green, J. C. Jeffery, J. E. McGrady, C. A. Russell, J. M. Slattery, A. C. Swain, Selective preparation of the 3,5-*t*Bu_2-1,2,4-C_2P_3-ion and synthesis and structure of the cationic species nido-3,5-*t*Bu_2-1,2,4-$C_2P_3^+$, isoelectronic with $C_5R_5^+$. *Angew. Chem. Int. Ed. Engl.* **42**, 2778–2782 (2003).
28. P. H. M. Budzalaar, IvorySoft: GNMR for Windows (2006).
29. M. Oberthür, Experiments in green and sustainable chemistry. Edited by Herbert W. Roesky and Dietmar Kennepohl. *Angew. Chem. Int. Ed.* **49**, 25 (2010).
30. G. R. Fulmer, A. J. M. Miller, N. H. Sherden, H. E. Gottlieb, A. Nudelman, B. M. Stoltz, J. E. Bercaw, K. I. Goldberg, NMR chemical shifts of trace impurities: Common laboratory solvents, organics, and gases in deuterated solvents relevant to the organometallic chemist. *Organometallics* **29**, 2176–2179 (2010).
31. R. K. Harris, E. D. Becker, S. M. Cabral de Menezes, R. Goodfellow, P. Granger, NMR nomenclature: Nuclear spin properties and conventions for chemical shifts: IUPAC Recommendations 2001. *Pure Appl. Chem.* **73**, 1795–1818 (2001).
32. A. Grodzicki, A. Potier, Spectroscopie de vibrations des ions $[Ga_2Br_7]^-$ et $[Ga_2Cl_7]^-$. *J. Inorg. Nucl. Chem.* **35**, 61–66 (1973).
33. C. S. Venkateswaran, The raman spectrum of phosphorus. *Proc. Indian Acad. Sci.* **2**, 260–264 (1935).
34. Oxford Diffraction/Agilent Technologies UK Ltd., CrysAlisPRO, Yarnton (GB) (2016).
35. O. Dolomanov, L. Bourhis, R. Gildea, J. Howard, H. Puschmann, OLEX2: A complete structure solution, refinement and analysis program. *J. Appl. Cryst.* **42**, 339–341 (2009).
36. G. M. Sheldrick, *SHELXT*—Integrated space-group and crystal-structure determination. *Acta Cryst A.* **71**, 3–8 (2015).
37. G. M. Sheldrick, Crystal structure refinement with SHELXL. *Acta Cryst C.* **71**, 3–8 (2015).
38. P. R. Spackman, M. J. Turner, J. J. McKinnon, S. K. Wolff, D. J. Grimwood, D. Jayatilaka, M. A. Spackman, CrystalExplorer: A program for Hirshfeld surface analysis, visualization and quantitative analysis of molecular crystals. *J. Appl. Cryst.* **54**, 1006–1011 (2021).
39. M. von Arnim, R. Ahlrichs, Performance of parallel TURBOMOLE for density functional calculations. *J. Comput. Chem.* **19**, 1746–1757 (1998).
40. O. Treutler, R. Ahlrichs, Efficient molecular numerical integration schemes. *J. Chem. Phys.* **102**, 346–354 (1995).
41. A. D. Becke, A new mixing of Hartree–Fock and local density-functional theories. *J. Chem. Phys.* **98**, 1372–1377 (1993).
42. A. D. Becke, Density-functional thermochemistry. III. The role of exact exchange. *J. Chem. Phys.* **98**, 5648–5652 (1993).
43. C. Lee, W. Yang, R. G. Parr, Development of the Colle-Salvetti correlation-energy formula into a functional of the electron density. *Phys. Rev. B* **37**, 785–789 (1988).
44. F. Weigend, R. Ahlrichs, Balanced basis sets of split valence, triple zeta valence and quadruple zeta valence quality for H to Rn: Design and assessment of accuracy. *Phys. Chem. Chem. Phys.* **7**, 3297–3305 (2005).
45. R. Ahlrichs, Efficient evaluation of three-center two-electron integrals over Gaussian functions. *Phys. Chem. Chem. Phys.* **6**, 5119 (2004).
46. M. Sierka, A. Hogekamp, R. Ahlrichs, Fast evaluation of the Coulomb potential for electron densities using multipole accelerated resolution of identity approximation. *J. Chem. Phys.* **118**, 9136–9148 (2003).
47. F. Weigend, Accurate Coulomb-fitting basis sets for H to Rn. *Phys. Chem. Chem. Phys.* **8**, 1057–1065 (2006).
48. S. Grimme, J. Antony, S. Ehrlich, H. Krieg, A consistent and accurate ab initio parametrization of density functional dispersion correction (DFT-D) for the 94 elements H-Pu. *J. Chem. Phys.* **132**, 154104 (2010).
49. S. Grimme, S. Ehrlich, L. Goerigk, Effect of the damping function in dispersion corrected density functional theory. *J. Comput. Chem.* **32**, 1456–1465 (2011).
50. P. Deglmann, F. Furche, R. Ahlrichs, An efficient implementation of second analytical derivatives for density functional methods. *Chem. Phys. Lett.* **362**, 511–518 (2002).
51. F. Neese, The ORCA program system. *WIRES Comput. Mol. Sci.* **2**, 73–78 (2012).
52. F. Neese, Software update: The ORCA program system, version 4.0. *WIRES Comput. Mol. Sci.* **8**, e1327 (2018).
53. F. Neese, F. Wennmohs, U. Becker, C. Riplinger, The ORCA quantum chemistry program package. *J. Chem. Phys.* **152**, 224108 (2020).
54. Y. Guo, C. Riplinger, U. Becker, D. G. Liakos, Y. Minenkov, L. Cavallo, F. Neese, Communication: An improved linear scaling perturbative triples correction for the domain based local pair-natural orbital based singles and doubles coupled cluster method [DLPNO-CCSD(T)]. *J. Chem. Phys.* **148**, 011101 (2018).
55. C. Riplinger, F. Neese, An efficient and near linear scaling pair natural orbital based local coupled cluster method. *J. Chem. Phys.* **138**, 034106 (2013).
56. C. Riplinger, B. Sandhoefer, A. Hansen, F. Neese, Natural triple excitations in local coupled cluster calculations with pair natural orbitals. *J. Chem. Phys.* **139**, 134101 (2013).
57. J. Chmela, M. E. Harding, Optimized auxiliary basis sets for density fitted post-Hartree–Fock calculations of lanthanide containing molecules. *Mol. Phys.* **116**, 1523–1538 (2018).
58. A. Hellweg, C. Hättig, S. Höfener, W. Klopper, Optimized accurate auxiliary basis sets for RI-MP2 and RI-CC2 calculations for the atoms Rb to Rn. *Theor. Chem. Acc.* **117**, 587–597 (2007).
59. F. Weigend, M. Kattannek, R. Ahlrichs, Approximated electron repulsion integrals: Cholesky decomposition versus resolution of the identity methods. *J. Chem. Phys.* **130**, 164106 (2009).
60. V. Barone, M. Cossi, Quantum calculation of molecular energies and energy gradients in solution by a conductor solvent model. *J. Phys. Chem. A* **102**, 1995–2001 (1998).
61. R. Izsák, F. Neese, An overlap fitted chain of spheres exchange method. *J. Chem. Phys.* **135**, 144105 (2011).
62. F. Neese, F. Wennmohs, A. Hansen, U. Becker, Efficient, approximate and parallel Hartree–Fock and hybrid DFT calculations. A 'chain-of-spheres' algorithm for the Hartree–Fock exchange. *Chem. Phys.* **356**, 98–109 (2009).
63. W. M. Haynes, D. R. Lide, T. J. Bruno, *CRC Handbook of Chemistry and Physics* (CRC Taylor & Francis, ed. 97, 2017).
64. M. Ligare, Classical thermodynamics of particles in harmonic traps. *Am. J. Phys.* **78**, 815–819 (2010).
65. H. Schmidbaur, Arene complexes of univalent gallium, indium, and thallium. *Angew. Chem. Int. Ed.* **24**, 893–904 (1985).

Acknowledgments: We would like to thank E. Hey-Hawkins for her very important contributions in the field of polyphosphorus chemistry, which contributed to this work. We thank S. Paasch for conducting the MAS NMR measurements, N. Kretzschmar for the pXRD measurements/calculations, N. Herold for the STA measurements, and B. Butschke for help with the Hirshfeld plots and fingerprint analysis. **Funding:** We thank the Technische Universität Dresden, the

University of Freiburg, the German Research Foundation [DFG, grant numbers WE4621/3-1 and WE4621/3-2 to J.J.W.; DFG, grant number KR2046/26-2 to I.K.; and DFG, grant numbers INST 40/467-1 and 575-1 FUGG (JUSTUS1 and JUSTUS2 cluster)], EC (ERC starting grant SynPhos 307616), and the State of Baden-Württemberg (bwHPC) for financial support. **Author contributions:** Conceptualization: J.F.-R., M.H., C.F., D.R., I.K., and J.J.W. Methodology: J.F.-R., M.H., C.F., D.R., I.K., and J.J.W. Investigation: J.F.-R., M.H., C.F., D.R., and J.J.W. Visualization: J.F.-R., C.F., D.R., I.K., and J.J.W. Funding acquisition: I.K. and J.J.W. Project administration: I.K. and J.J.W. Supervision: I.K. and J.J.W. Writing—original draft: J.F.-R., C.F., D.R., I.K., and J.J.W. Writing—review and editing: J.F.-R., C.F., D.R., I.K., and J.J.W. **Competing interests:** The authors declare that they have no competing interests. **Data and materials availability:** All data needed to evaluate the conclusions in the paper are present in the paper and/or the Supplementary Materials. Crystallographic data have been deposited in the Cambridge database. CCDC 2166039- 2166043 contain the supplementary crystallographic data for this paper. These data can be obtained free of charge from the Cambridge Crystallographic Data Centre at www.ccdc.cam.ac.uk/data_request/cif.

Submitted 5 May 2022
Accepted 26 July 2022
Published 7 September 2022
10.1126/sciadv.abq8613